

Use of MR Cell Tracking to Evaluate Targeting of Glial Precursor Cells to Inflammatory Tissue by Exploiting the Very Late Antigen-4 Docking Receptor¹

Michael Gorelik, BS
Inema Orukari, BS
Joanne Wang, PhD
Shashikala Galpotthawela, BS
Heechul Kim, PhD
Michael Levy, MD, PhD
Assaf A. Gilad, PhD
Amnon Bar-Shir, PhD
Douglas A. Kerr, MD, PhD²
Andre Levchenko, PhD
Jeff W. M. Bulte, PhD
Piotr Walczak, MD, PhD

¹From the Russell H. Morgan Department of Radiology and Radiological Science, Division of MR Research (M.G., I.O., S.G., H.K., A.A.G., A.B.S., J.W.M.B., P.W.), Cellular Imaging Section and Vascular Biology Program, Institute for Cell Engineering (M.G., I.O., J.W., S.G., H.K., A.A.G., A.B.S., A.L., J.W.M.B., P.W.), Department of Biomedical Engineering (J.W., A.L., J.W.M.B.), Department of Chemical & Biomolecular Engineering (J.W.M.B.), and Department of Neurology (M.L., D.A.K.), The Johns Hopkins University School of Medicine, 733 N Broadway, Broadway Research Building, Room 649, Baltimore, MD 21205. Received October 17, 2011; revision requested December 8; revision received April 11, 2012; accepted April 25; final version accepted May 3. Supported by Maryland Stem Cell Research grants MSCRF110193 and MSCRF110190. Address correspondence to P.W. (e-mail: pwalczak@mri.jhu.edu).

²Current address: Biogen-IDEC, Cambridge, Mass.

© RSNA, 2012

Purpose:

To determine if glial precursor cells can be targeted to inflamed brain through overexpression of very late antigen-4 (VLA-4) and whether this docking process can be monitored with magnetic resonance (MR) cell tracking after intraarterial injection.

Materials and Methods:

All experimental procedures were performed between August 2010 and February 2012 and were approved by the institutional animal care and use committee. Human glial precursor cells (hGPs) were transfected with VLA-4 and labeled with superparamagnetic iron oxide that contained rhodamine. A microfluidic adhesion assay was used for assessing VLA-4 receptor-mediated cell docking in vitro. A rat model of global lipopolysaccharide (LPS)-mediated brain inflammation was used to induce global vascular cell adhesion molecule-1 (VCAM-1) expression. hGPs were infused into the carotid artery in four animal cohorts (consisting of three rats each): rats that received VLA-4-naïve hGPs but did not receive LPS, rats that received VLA-4-expressing hGPs but not LPS, rats that received VLA-4-naïve hGPs and LPS, and rats that received VLA-4-expressing hGPs and LPS. MR imaging was performed at 9.4 T before and 1, 10, 20, and 30 minutes after injection. Brain tissue was processed for histologic examination. Quantification of low-signal-intensity pixels was performed with pixel-by-pixel analysis for MR images obtained before and after cell injection.

Results:

With use of the microfluidic adhesion assay, cell binding to activated brain endothelium significantly increased compared with VLA-4-naïve control cells (71.5 cells per field of view \pm 11.7 vs 36.4 cells per field of view \pm 3.3, respectively; $P < .05$). Real-time quantitative in vivo MR cell tracking revealed that VLA-4-expressing cells docked exclusively within the vascular bed of the ipsilateral carotid artery and that VLA-4-expressing cells exhibited significantly enhanced homing as compared with VLA-4-naïve cells (1448 significant pixels \pm 366.5 vs 113.3 significant pixels \pm 19.88, respectively; $P < .05$). Furthermore, MR cell tracking was crucial for correct cell delivery and proper ligation of specific arteries.

Conclusion:

Targeted intraarterial delivery and homing of VLA-4-expressing hGPs to inflamed endothelium is feasible and can be monitored in real time by using MR imaging in a quantitative, dynamic manner.

© RSNA, 2012

Supplemental material: <http://radiology.rsna.org/lookup/suppl/doi:10.1148/radiol.12112212/-/DC1>

Successful cell-based therapy of neurologic disease depends on the efficient delivery of cells to regions of central nervous system abnormality. Intraparenchymal stereotaxic injection is currently the most prevalently used technique for cell delivery to the central nervous system in animal models (1) and clinical trials (2,3). However, intraparenchymal injections are invasive, can lead to nonuniform cell engraftment, and result in limited brain area coverage by the graft. Intravenous systemic cell administration has been proposed as a less-invasive delivery route to ensure a broad cell distribution (4). The challenge with this intravenous approach is achieving specific, high-efficiency binding to target regions in the central nervous system. Typically, with intravenous injection, the vast majority of infused cells become trapped in filtering organs (5). An alternative method of intravascular delivery is to target the cells to an artery that directly feeds the defunct region. It has been shown that intraarterial delivery can result in increased cell engraftment to brain lesions (6) and, notably, fewer cells found in off-target organs. Furthermore, there is evidence that intraarterial delivery results in modest functional recovery in animal models of stroke (7) and brain trauma (8).

Advances in Knowledge

- Transient expression of the adhesion molecule very late antigen-4 (VLA-4) by glial precursor cells results in their enhanced binding to inflamed brain endothelium both *in vitro* (71.5 cells per field of view \pm 11.7 vs 36.4 cells per field of view \pm 3.3, determined with microfluidic assay) and *in vivo* (1448 significant pixels \pm 366.5 vs 113.3 significant pixels \pm 19.88, determined with low signal intensities).
- Docking of superparamagnetic iron oxide–labeled and VLA-4–transfected cells to brain endothelium can be monitored and quantified in real time with cellular MR imaging.

A limitation of current intraarterial delivery methods using nonengineered cells is highly variable (9) and inefficient engraftment. With nonengineered cells, only a small fraction of cells accumulate within the lesion site. In addition, many cells that initially engraft are lost within a few days after infusion (10). One strategy to improve engraftment efficiency is to transplant cells with endogenous expression of adhesion molecules (11). However, this would severely limit the cell types available for this procedure because many stem and precursor cells do not express the appropriate adhesion molecules. Genetically engineering cells to express specific adhesion molecules offers a more versatile approach in which a specific pattern of adhesion molecules could be temporarily induced and customized as needed for particular lesion targeting. In combination with intraarterial delivery, this approach would allow more specific targeting to areas of abnormality, improve existing intraarterial methods, and potentially overcome the limitations of direct stereotaxic and intravenous cell delivery.

One of the most relevant cell adhesion pathways that can be exploited for stem cell targeting is the well-characterized very late antigen-4 (VLA-4)–vascular cell adhesion molecule-1 (VCAM-1) adhesion pathway used by trafficking leukocytes (12). The expression of VLA-4 on leukocytes allows them to anchor to the endothelium in the proximity of the brain lesion, respond to chemokine-mediated signaling, cross the blood-brain barrier, and migrate to areas of neuroinflammation. VLA-4, a heterodimer consisting of the α_4 and β_1 integrin subunits, signals leukocytes to bind to VCAM-1 on inflamed endothelial tissues and subsequently extravasate into the central nervous system parenchyma by means of a process called diapedesis (13). We hypothesized that exogenous overexpression of VLA-4 in migratory glial precursor cells would allow these cells to bind to immunoinactivated cerebral endothelium as a first step in the process of responding to chemokine signals and extravasation into the brain parenchyma. However, although such



increased adhesion is highly desired for intraarterial infusion of cells, this approach may potentially amplify the risk of the formation of microembolisms (6,9), compromising essential cerebral blood flow. Thus, to ensure the safety of this approach, it is crucial to monitor cell delivery noninvasively in real time. The use of *in vivo* magnetic resonance (MR) imaging with superparamagnetic iron oxide (SPIO) nanoparticle–labeled cells, which is now used clinically (14), enables real-time visualization of both correct cell delivery (15,16) and the relative amount of cell engraftment (9). The purpose of this study was to determine if glial precursor cells can be targeted to inflamed brain through overexpression of VLA-4 and whether this docking process can be monitored with MR cell tracking after intraarterial injection.

Materials and Methods

Cell Preparation

Immortalized human glial precursor cells (hGPs) were maintained in Dulbecco's modified Eagle's medium: nutrient

Published online before print

10.1148/radiol.12112212 Content codes:  

Radiology 2012; 265:175–185

Abbreviations:

hGP = human glial precursor cells

LPS = lipopolysaccharide

SPIO = superparamagnetic iron oxide

TNF- α = tumor necrosis factor- α

VCAM-1 = vascular cell adhesion molecule-1

VLA-4 = very late antigen-4

Author contributions:

Guarantors of integrity of entire study, J.W.M.B., P.W.; study concepts/study design or data acquisition or data analysis/interpretation, all authors; manuscript drafting or manuscript revision for important intellectual content, all authors; manuscript final version approval, all authors; literature research, M.G., M.L., J.W.M.B., P.W.; experimental studies, M.G., I.O., J.W., H.K., M.L., A.A.G., A.B., D.A.K., A.L., J.W.M.B., P.W.; statistical analysis, M.G., I.O., J.W., A.L., J.W.M.B., P.W.; and manuscript editing, M.G., J.W., S.G., M.L., D.A.K., A.L., J.W.M.B., P.W.

Funding:

This research was supported by the National Institutes of Health (grant NIH 2R01 NS045062).

Potential conflicts of interest are listed at the end of this article.

See also Science to Practice in this issue.

mixture F-12 (Life Technologies, Grand Island, NY) supplemented with basic-FGF, B-27, and N2 (Life Technologies). Forty-eight hours before cell infusion, hGPs were cotransfected with the α_4 and β_1 subunits of VLA-4 integrin (GeneCopoeia, Rockville, Md) by using Lipofectamine 2000 (Life Technologies, 4 μ L/mL). Twenty-four hours before cell infusion, VLA-4-transfected and control cells were labeled with SPIO-rhodamine nanoparticles (Molday ION; Biopal, Worcester, Mass), allowing MR imaging visualization and cell detection with microscopy owing to red fluorescence. Expression of VLA-4 was confirmed with immunocytochemistry against each integrin subunit (α_4 ; R&D Systems, Minneapolis, Minn; β_1 ; Santa Cruz Biotechnology, Santa Cruz, Calif), enabling quantification of the relative fluorescence for transfected and nontransfected cells. The efficiency of SPIO uptake was assessed with fluorescent microscopy, with labeling considered satisfactory when almost 100% of cells showed internalized red fluorescent particles. On the day of transplantation, cells were harvested by using Accutase (Sigma, St Louis, Mo), passed through a 40- μ mol/L filter (BD Biosciences, San Jose, Calif), and resuspended at 2×10^6 cells per milliliter.

Microfluidic Cell Adhesion Assay

A custom microfluidic device was designed for in vitro validation of the VLA-4-VCAM-1 pathway and to provide a method by which to model the interaction of cells within capillaries. Polydimethylsiloxane channels were coated with fibronectin (10 μ g/mL, Life Technologies) for 1 hour and seeded with human brain endothelial cells. Cells were allowed to form a monolayer for 24 hours in normal growth medium or a medium supplemented with tumor necrosis factor- α (TNF- α , 10 ng/mL, R&D Systems). Twenty-four hours before the adhesion experiment, hGPs were labeled with Molday ION for fluorescence visualization. A rolling adhesion assay was conducted at physiologic wall shear stresses of 0.1 Pa for 10 minutes. Unattached cells were washed out with medium. Adhesion was analyzed under four conditions comparing

VLA-4-expressing or nonexpressing hGPs binding to naive or TNF- α -treated endothelial cells. At the end of each flow experiment, cells were subjected to excessive shear stress of more than 0.2 Pa elicited by increased flow velocity for several seconds. The purpose of this test was to determine the effect of VLA-4 expression on the strength of cell adhesion. Imaging was performed by using an automated epifluorescent microscope. The entire channel surface was photographed with use of phase-contrast and rhodamine filters. Merged images were digitally stitched together, and the total number of adherent hGPs was determined. Cell culture work and in vitro assays were performed by M.G., I.O., S.G. (each with 2 years of experience with cell cultures), and H.K. (with 8 years of experience with cell cultures and in vitro assays). Adhesion assays and cell counting were performed by J.W. (with 4 years of experience with these assays).

Animal Studies

All experimental procedures were performed between August 2010 and February 2012 and were approved by our institutional animal care and use committee. Adult female Lewis rats (Charles River Laboratories, Wilmington, Mass) weighing 200–220 g were housed under an artificial 12 hour light–12 hour dark cycle with access to food and water ad libitum. Twenty-four hours before cell infusion, rats ($n = 9$) received intraperitoneal injection of 6 mg/kg lipopolysaccharide (LPS) for global induction of VCAM-1 expression. Isoflurane-anesthetized animals were placed in the supine position, and the common carotid artery was cannulated as previously described (9). The pterygopalatine artery was ligated after initial experiments demonstrated that cells were infused extracerebrally without this procedure ($n = 3$). Four experimental conditions were evaluated in three rats each, including combinations of naive and LPS-treated rats that received either VLA-4-expressing or naive hGPs (2×10^6 cells in 1 mL). The four animal cohorts were as follows: rats that received VLA-4-naive

hGPs but not LPS (VLA-4-/LPS-), rats that received VLA-4-expressing hGPs but not LPS (VLA-4+/LPS-), rats that received VLA-4-naive hGPs and LPS (VLA-4-/LPS+), and rats that received VLA-4-expressing hGPs and LPS (VLA-4+/LPS+). The first three groups represented controls for the VLA-4+/LPS+ group. Once cannulation was performed, the rats were transferred to the MR unit to monitor the engraftment of magnetically labeled hGPs. Animal experiments were performed by M.G., I.O., and P.W.

MR Imaging

Animals were positioned in a custom-built 35-mm volume coil and placed inside a 9.4-T MR unit (Bruker, Billerica, Mass). Polytetrafluoroethylene tubing extending outside the MR unit enabled cell infusion without repositioning of the animal. Five sets of T2*-weighted images (repetition time msec/echo time msec = 300/4, two signals acquired, four repetitions, 200×200 - μ m resolution) were obtained for each animal (a) before cell injection, (b) 1 minute after injection of 1×10^6 cells, (c) after a second injection of 1×10^6 cells, and (d) 10 and 20 minutes after administration of the second cell injection. A two-injection paradigm was used to demonstrate the applicability of MR monitoring of multiple cell injections.

Histologic Analysis

Immediately after MR imaging, rats were transcardially perfused with phosphate-buffered saline (pH = 7.4) followed by 4% paraformaldehyde. Brains were removed and postfixed for 24 hours in 4% paraformaldehyde, cryopreserved in a 30% sucrose solution, and flash frozen. Axial tissue sections were cut into 30- μ m-thick slices and processed to detect transplanted cells. Primary antibodies used in this study were antihuman nuclei (Millipore, Billerica, Mass), anti-von Willebrand factor (DAKO, Carpinteria, Calif), anti-VCAM-1 (Serotec, Raleigh, NC), anti- α_4 (R&D Systems), and anti- β_1 (Santa Cruz Biotechnology). Histologic analysis was performed with immunostaining (S.G.,

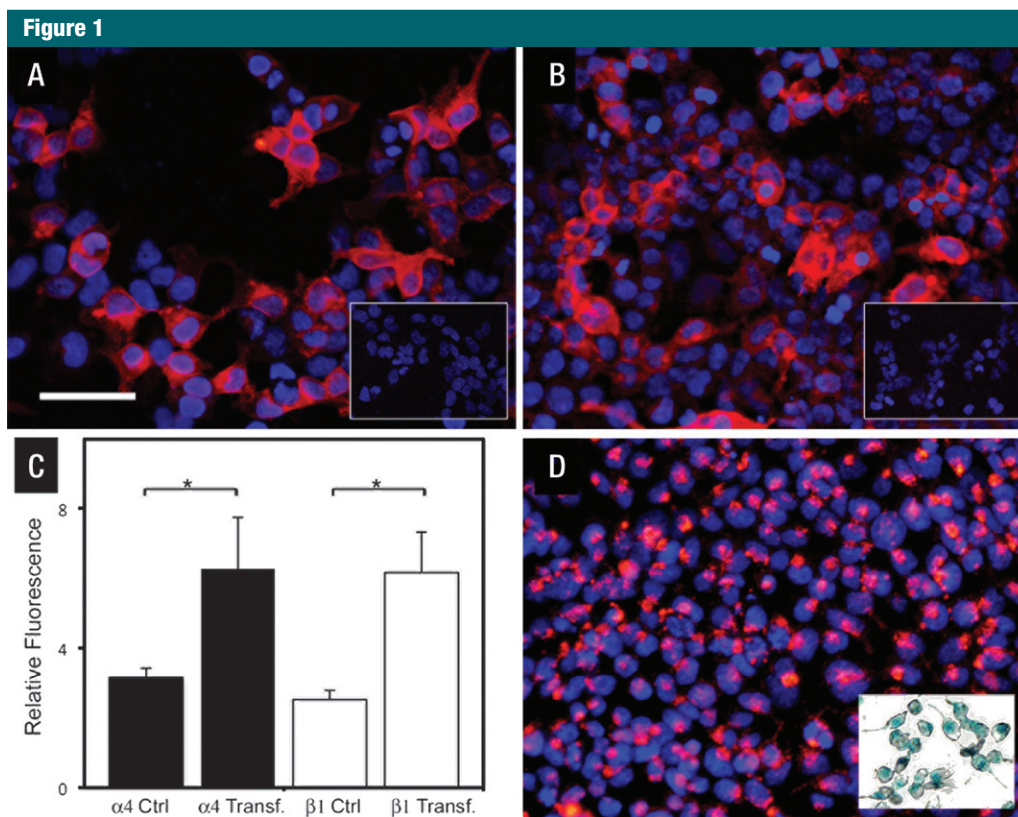


Figure 1: VLA-4 gene expression and SPIO labeling: characterization with immunofluorescence microscopy. *A, B*, Immunofluorescence images show that transfected glial precursors highly express VLA-4 subunits α_4 (*A*, red) and β_1 (*B*, red). Basal expression in nontransfected cells was very low (insets). *C*, Bar chart shows quantification of relative fluorescence. Data are means \pm standard deviations, with * indicating significant difference between groups. *Ctrl* = control cells, *Transf.* = transfected cells. *D*, Immunofluorescence image shows that labeling of hGPs with fluorescent iron oxide nanoparticles results in internalization of contrast agent with a characteristic perinuclear distribution. Red fluorescence corresponded well with Prussian blue staining for iron (inset). Nuclei are counterstained with 4,6-diamidino-2-phenylindole (blue). Scale bar in *A* is 50 μ m and applies to all immunofluorescence images.

3 years of experience) and fluorescent microscopy (with image analysis performed in consensus by M.G., H.K., and P.W., each with 8 years of experience).

MR Imaging Processing

Quantification of pixels with low signal intensity after injection of SPIO-labeled cells (hypointense to pixels on preinjection baseline images) was performed by using software (MatLab; MathWorks, Natick, Mass). Regions of interest were specified by using a custom-written script and drawn for every image to cover the entire brain area. A pixel-by-pixel analysis was conducted for images obtained before cell injection and 20 minutes after the second injection. A *t*

test was performed for each pixel, comparing four repetition images before injection to four images after injection. Pixels with $P < .001$ were designated as hypointense. This value was heuristically chosen because it was the conventional *P* value that provided the best balance between hypointense pixel coverage and specificity. The total number of hypointense pixels per animal was quantified in each animal group. Image processing was done in consensus by I.O., A.A.G., and A.B.

Statistical Analysis

Analysis of variance was performed by using the Tukey test for comparisons between groups, with the significance

level set at $\alpha = .05$ (Proc ANOVA; SAS Institute, Cary, NC).

Results

Overexpression of VLA-4 in hGPs Assessed with Microfluidic Adhesion Assay

Following VLA-4 transfection, we observed a wave of expression, with the maximum occurring after 48 hours (Fig 1). Immunoreactivity was predominantly localized on the plasma membrane, indicating an appropriate expression routing of the ligand. Quantification of fluorescence intensity in fixed cells immunostained for α_4 and

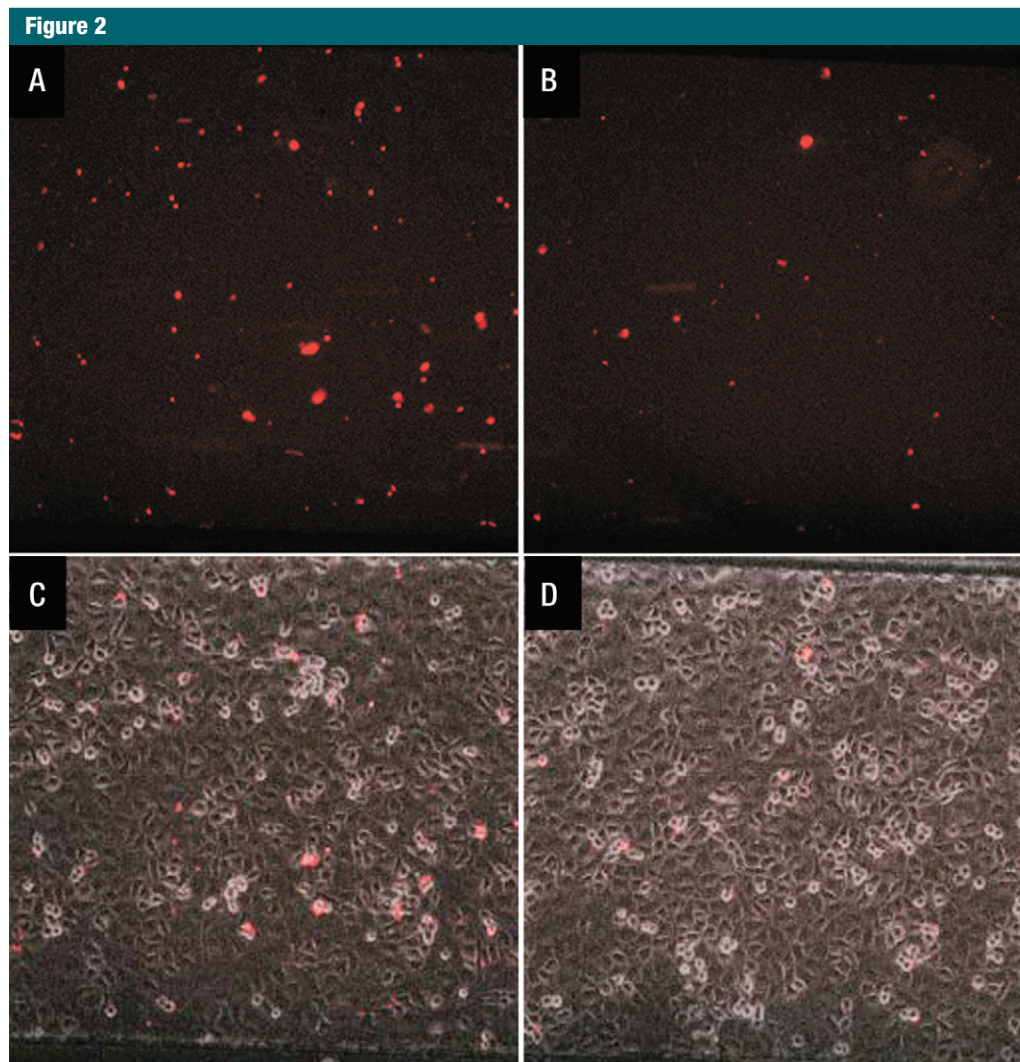


Figure 2: Functional VLA-4 gene expression: characterization with microfluidic adhesion assay. Fluorescent photomicrographs from a microfluidic device coated with TNF- α -treated endothelial cells. *A, B*, Images show in vitro docking for red fluorescent VLA-4-expressing glial precursor cells (*A*) and VLA-4-naive control cells (*B*). Much greater endothelial adhesion was observed for VLA-4-engineered cells. *C, D*, Overlays of phase-contrast and fluorescent images show dense coating of the microfluidic device with endothelial cells. Images were acquired with $\times 10$ objective.

β_1 (Fig 1, *C*) revealed that the transfection resulted in a significant overexpression of both molecules in comparison to the controls ($df = 3$, $F = 24.5$, $P < .001$). Next, we sought to evaluate the functionality of the introduced docking molecule by using a microfluidic adhesion assay (17). Labeling with SPIO was highly efficient for both naive and VLA-4-overexpressing cells, with all the cells positive and the contrast agent localized within the cytosol (Fig 1, *D*). Fluorescently labeled cells were

perfused into microfluidic chambers (17) seeded with naive or TNF- α -activated human brain endothelial cells. With this assay, we demonstrated that VLA-4 expression on hGPs led to a dramatic enhancement of cell binding, with the greatest effect observed for TNF- α -treated endothelial cells (Figs 2, 3; Movies 1, 2 [online]). End-point analysis after 20 minutes of perfusion revealed a significantly higher degree of binding of VLA-4-expressing cells to TNF- α -activated endothelial cells

compared with all control cells ($df = 3$, $F = 37.31$, $P < .001$) (Figs 2, 3), indicating that VLA-4 transfection led to approximately twofold enhancement of cell capture. Notably, when the flow velocity was increased, naive cells (VLA-4-/TNF- α +) that initially adhered were detached and washed away, indicating weak cell-cell binding (Movie 3 [online]). Conversely, VLA-4-expressing cells remained strongly adhered to TNF- α -treated endothelium under increased flow velocity,

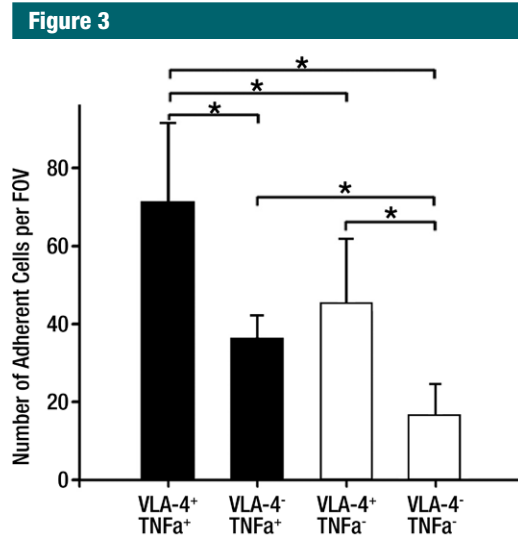


Figure 3: Bar chart shows quantification of microfluidic assay data. Endpoint quantification of the number of glial precursor cells that adhered to endothelium-coated microfluidic device demonstrates a significant increase in cell adhesion for VLA-4-expressing cells. The greatest increase was observed for VLA-4-expressing cells and TNF- α -treated endothelial cells. Data are means \pm standard deviations. * = Significant difference between groups.

displaying some degree of rolling but no detachment (Movie 4 [online]).

Monitoring Cell Delivery with Real-Time MR Imaging

In a pilot experiment where the pterygopalatine artery was left intact, we observed that the vast majority of infused SPIO-labeled cells were targeted to tissue located outside of the brain (Fig 4). Ligation of all internal carotid artery extracerebral branches prevented cells from being targeted to regions outside of the brain. Subsequent cell targeting experiments were performed after these ligations with two bolus injections of 1×10^6 cells given 10 minutes apart. MR imaging demonstrated that VLA-4-expressing hGPs injected into animals treated with LPS bind extensively to the cerebral endothelium, as represented by low-signal-intensity pixels, whereas control experiments with VLA-4-naïve cells or naïve endothelium (not treated with LPS) were associated with much fewer signals (Fig 5). As a quantitative measure of intracerebral cell binding, a pixel-by-pixel *t* test was conducted

in which the signal intensity of pixels within the entire brain area on the MR images obtained before injection was compared with that on the end-point images. Pixels with a statistically significant decrease in signal intensity were present throughout the ipsilateral hemisphere. Quantitative analysis (Fig 6) revealed that injection of VLA-4-expressing cells in animals treated with LPS resulted in 1448 significant pixels \pm 366.5 compared with 113.3 significant pixels \pm 19.88, 402.7 significant pixels \pm 188.7, and 129.2 significant pixels \pm 74.59 for the three control groups VLA-4-/LPS+, VLA-4+/LPS-, and VLA-4-/LPS-, respectively. Statistical analysis proved a significant increase of cell homing for animals in the VLA-4+/LPS+ group compared with the three control groups ($df = 3$, $F = 8.53$, $P = .007$).

Validation of Imaging Findings with Histologic Results

Immunostaining for VCAM-1 demonstrated global, high-level expression of VCAM-1 within the brain of rats treated with LPS (Fig E1, a [online]). In

naïve animals, VCAM-1 expression was low (Fig E1, b [online]). This characteristic pattern of staining indicates that VCAM-1 upregulation occurred in brain vasculature, providing a proper adhesion platform for our engineered cells. In animals with LPS-induced inflammation that were injected with VLA-4-expressing cells labeled with rhodamine-SPIO, there was an abundance of cells throughout the ipsilateral hemisphere (Fig 7, B). The distribution of adherent cells at histopathologic examination was in good agreement with the hypointense areas seen on the MR imaging pixel maps. Cells were localized within the von Willebrand factor-positive blood vessels (Fig 7, C). Conversely, although occasional examples were found, there was a near absence of injected cells in the ipsilateral hemisphere of control groups. The extremely low number of cells in the contralateral hemisphere for all groups, including VLA-4+/LPS+ (Fig 7, A), indicates that cells entering the circulation are trapped in filtering organs and do not reenter the brain.

Discussion

In our study, we demonstrated that transient VLA-4 overexpression in hGPs leads to an increase in their ability to bind to TNF- α -induced inflamed brain endothelium as shown *in vitro* by using a microfluidic adhesion assay. These results were confirmed *in vivo* in a rat model of global inflammation, in which we showed that VLA-4-expressing hGPs infused into the carotid artery bind extensively to activated endothelium. Finally, we demonstrated that the process of intraarterial cell delivery could be monitored by using real-time, quantitative, serial whole-brain MR imaging of magnetically labeled cells and that this MR imaging visualization prompted us to ligate the arteries branching off from the carotid artery to ensure proper cerebral targeting.

Beneficial outcomes of cell-based therapy are highly dependent on the efficient and safe delivery of cellular therapeutics to brain lesions. Widespread and targeted cell engraftment is particularly important for diseases

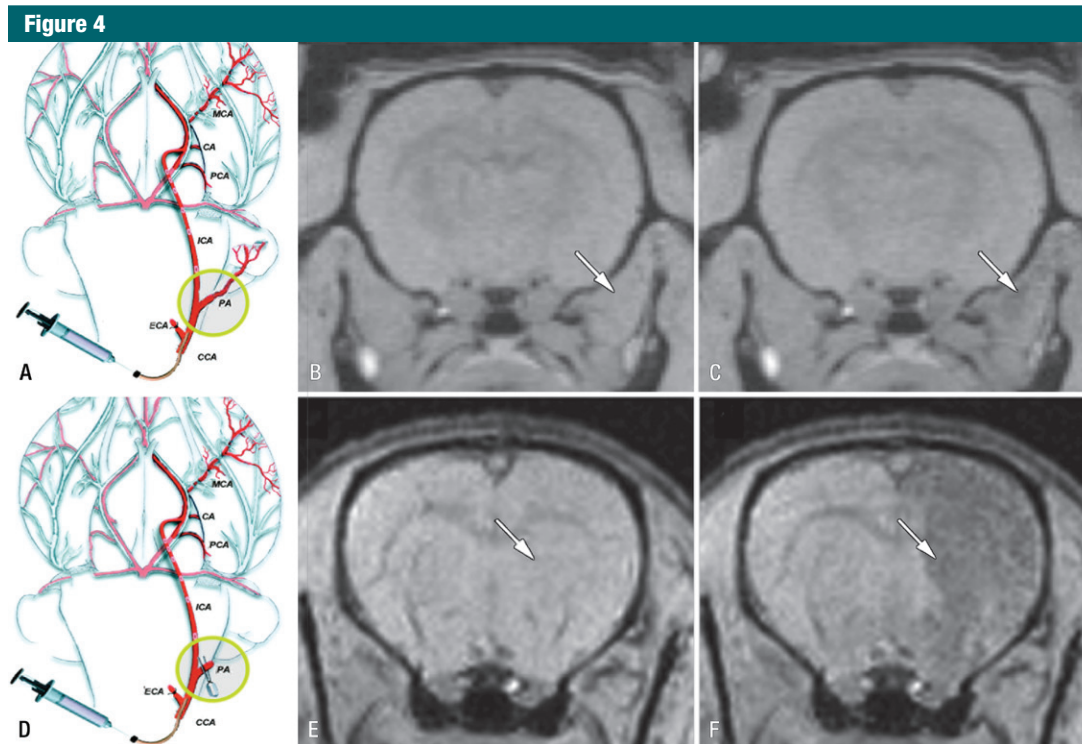


Figure 4: Real-time monitoring of injection accuracy with MR imaging. *A*, Diagram of procedure with pterygopalatine artery left intact. After ligation of external carotid and occipital arteries, common carotid artery was cannulated and SPIO-labeled cells were infused. *B*, *C*, MR images of rat brain and surrounding muscles obtained immediately before (*B*) and after (*C*) injection demonstrate that vast majority of cells are localized into extracerebral tissue (arrows), with negligible binding within brain. *D*, Diagram of procedure with ligation of pterygopalatine artery. All infused cells were perfused into internal carotid artery and localized successfully into ipsilateral hemisphere. *E*, *F*, MR images obtained immediately before (*E*) and after (*F*) injection. Arrows indicate area of cell docking. CA = choroidal anterior artery, CCA = common carotid artery, ECA = external carotid artery, ICA = internal carotid artery, MCA = middle cerebral artery, PA = pterygopalatine artery, PCA = posterior cerebral artery.

with multifocal or diffuse abnormalities. Such broad engraftment can be achieved either by relying on the extensive migratory potential of cells or with a delivery method that ensures cell placement in the immediate proximity of the affected tissue. Stereotaxic methods are efficacious for diseases in which the abnormality is focal or limited in extent. These methods have been used extensively in animal models (18) as well as in clinical trials for Parkinson disease (19), Huntington disease (20), and amyotrophic lateral sclerosis (21). However, although certain cell types have extensive migratory potential (18) with intraparenchymal injection, uniform and complete coverage of larger or multifocal lesions is challenging (22). For instance, in multiple sclerosis, a demyelinating disease

with lesions throughout the brain and spinal cord (23), comprehensive cell therapy would require multiple injections, which cannot be considered owing to excessive risk. Intravenous approaches to cell delivery have been used in animal models and clinical trials (14,24), with reassuring results in terms of safety parameters. However, although intravenous approaches are potentially safer and less invasive than stereotaxic methods, there are serious concerns about the low efficiency of engraftment (as low as 1%–2%) (25). It is difficult to control cell trafficking with this approach, and many reports indicate that transplanted cells filter into off-target organs such as the lungs or spleen (5,26). Finally, given the cost and difficulty of obtaining high-quality cells, this approach may

pose a substantial financial burden. Intraarterial cell delivery potentially addresses some of the limitations of both stereotaxic and intravenous methods. A major advantage of intraarterial delivery stems from the potential of widespread engraftment, which is essential for covering larger or multifocal lesions, as well as high targeting efficiency. This approach is valid only for cells that highly express adhesion-docking molecules, ensuring first-pass binding and minimizing cells from reaching off-target tissues. Expression of adhesion molecules in some cell types such as mesenchymal stem cells is quite high (27), whereas in neural cell types this expression is not consistent (28). It has been reported by Guzman et al (11) that neural stem cells could be enriched for cells with

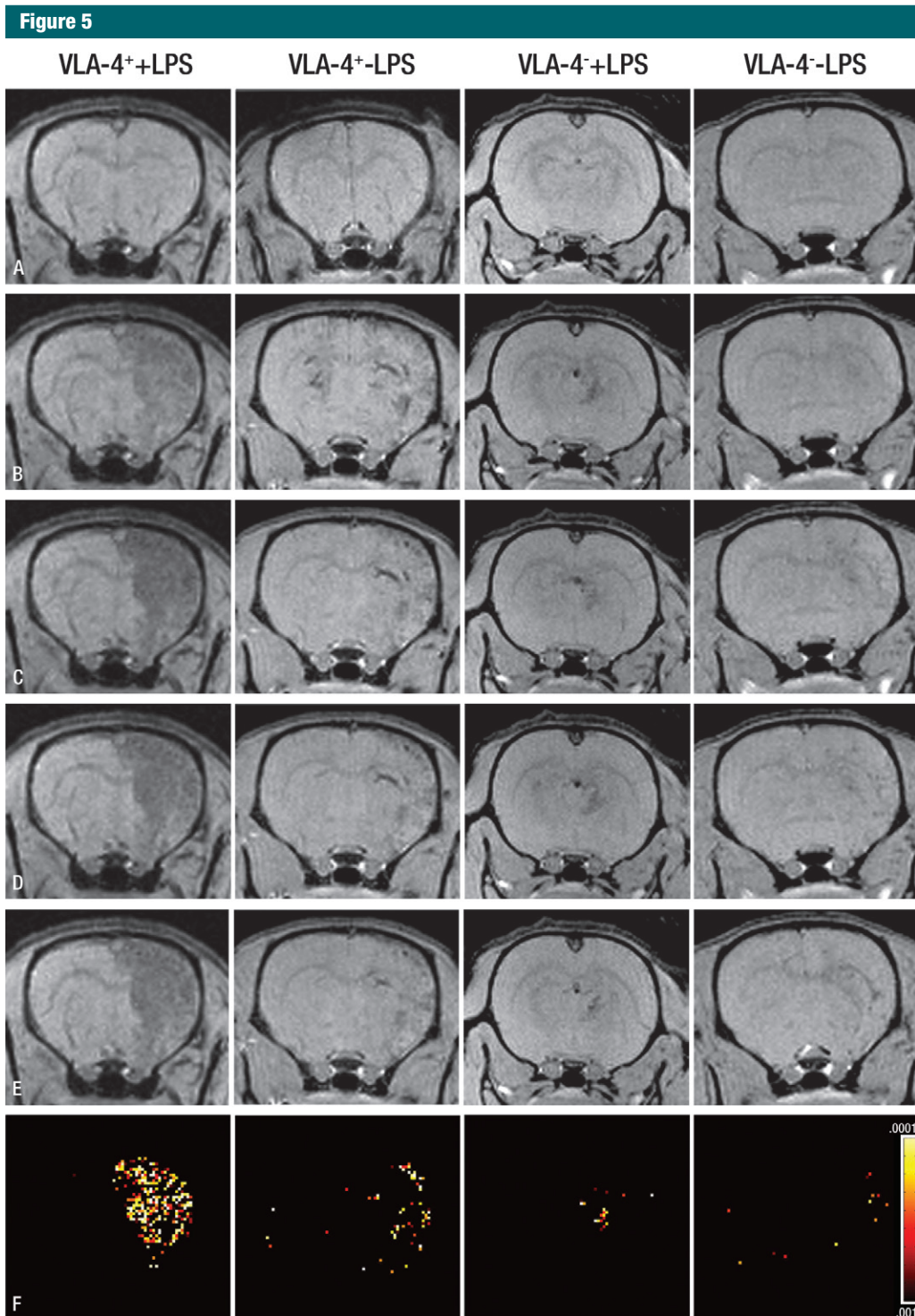


Figure 5: In vivo real-time quantitative MR images of cerebral docking of cells. Representative T2*-weighted brain images for all experimental groups acquired, *A*, before injection, *B*, after injection of 1×10^6 cells, *C*, 10 minutes later after second injection of 1×10^6 cells, and, *D*, 20 minutes and, *E*, 30 minutes after first injection. Brain regions with low signal intensity indicate docking of cells to cerebral endothelium. *F*, Pixel-by-pixel analysis of preinjection MR images (*A*) versus those obtained 30 minutes after first injection (*E*), with a significance threshold of $P < .001$. A larger number of hypointense pixels are seen for VLA-4-expressing cells after LPS treatment.

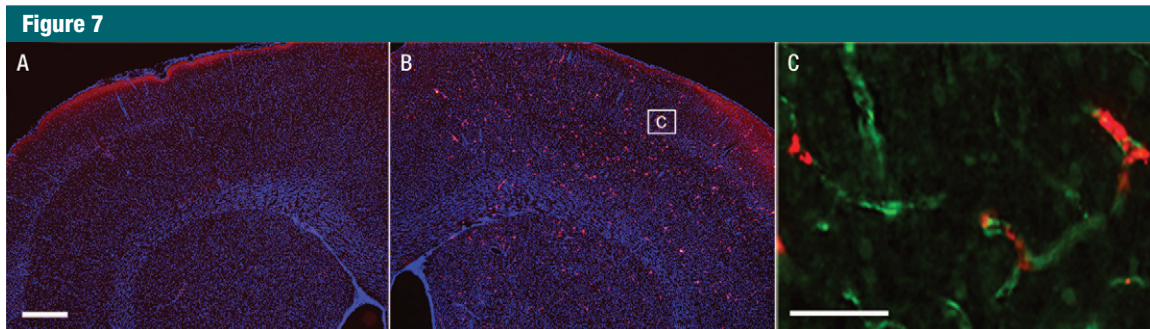


Figure 7: Validation of imaging results with immunofluorescent microscopy. *A*, Contralateral and, *B*, ipsilateral hemispheres of rats treated with LPS and injected with VLA-4-expressing hGPs reveal numerous red fluorescent cells (labeled with rhodamine-SPIO) only for the hemisphere located at site of intracarotid injection. *C*, Immunostaining for VLA-4-expressing hGPs (red, labeled with rhodamine-SPIO) and blood vessels (green, von Willebrand factor) shows binding of VLA-4-expressing hGPs to brain endothelium in the cortex (boxed *c* in *B*). Scale bar in *A* = 500 μ m; scale bar in *C* = 50 μ m.

Figure 6

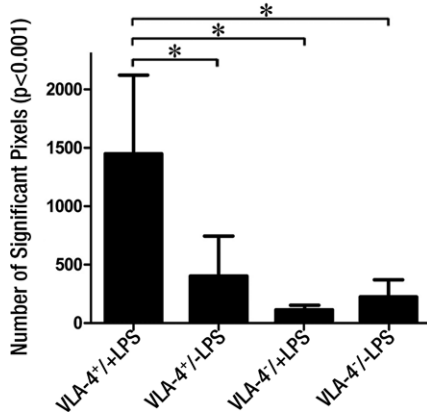


Figure 6: Bar chart shows quantification of numbers of hypointense pixels between VLA-4+/LPS+ and control groups. Data are means \pm standard deviations. * = Significant difference between groups.

greater expression of adhesion molecules and that these cells could later be infused into the carotid artery. However, their analysis revealed that only 25% of their cell population expressed the relevant molecule. Cell engineering to overexpress these types of adherins presents a more successful path forward. For cell types with low endogenous expression of adhesion receptors, it is crucial to artificially increase their presence by using a variety of approaches that range from stable expression systems (eg, lentiviral vectors) to transient expression

systems (eg, plasmid transfections or RNA-based technology). However, given the risks of stable genome integration, short-term expression may be a safe and more desirable method.

Selection of the appropriate adhesion pathway is crucial for maximizing the therapeutic potential of intraarterial delivery with engineered cells. A variety of integrins are upregulated on activated endothelium, and these molecules mediate rolling, adhesion, and extravasation of migrating cells. These molecules include a variety of selectins that mediate weaker binding and integrins, such as VCAM-1 and intracellular adhesion molecule-1, which mediate the strong binding that is crucial for extravasation. Thus, the use of a well-characterized cell adhesion pathway for intraarterial delivery offers the benefit of specific targeting to areas of abnormality. Furthermore, expression of adhesion receptors on therapeutic cells can be tailored for various diseases, with a characteristic expression profile of adhesion molecules. For instance, the VLA-4-VCAM-1 pathway can be used for cell targeting in a variety of central nervous system diseases such as multiple sclerosis (29) or stroke (30). Administration of engineered cells would not only facilitate widespread engraftment but would also improve the efficiency of binding to areas where cellular therapeutics would have the most significant effect. However, it must be noted that cell extravasation across

the blood-brain barrier is a complex molecular process that involves a host of adhesion molecules and chemokine receptors. Thus, we must determine which cell types are capable of homing toward areas of abnormality. Although successful docking of injected cells, as shown herein, is a prerequisite and the most important aspect of cells able to reach specific areas of neuropathologic lesions, additional receptor expression may be needed for molecules that promote cellular diapedesis and targeted migration (eg, CXCR-4 [31,32] or CCR-2 [33]). In the meantime, our approach may also be applied to “diagnose” inflammation in a similar fashion to the way indium 11-labeled leukocytes are used for specific imaging of inflammation and infection. When combined with a therapeutic effect, these targeted cells could then be considered to be a “theranostic” entity.

Our study has limitations. Intraarterial delivery of therapeutic cells can be associated with the risk of microembolism. Although applied here MR cell tracking can help monitor the overall amount of cell engraftment, this technique does not provide information about the physiologic status of brain tissue such as perfusion and oxygenation. An additional limitation is that we used xenogeneic cells for transplantation as a proof of principle, without having studied any potential long-term complications arising from a possible immune rejection. We have evaluated only the

immediate vascular adhesion of VLA-4-transfected cells, and further studies on subsequent extravasation must be conducted.

Intraarterial delivery of therapeutic cells can potentially lead to excessive cell binding and compromised blood flow (6,9), although several groups have shown evidence to the contrary (34). Given these safety concerns, we must address the need to balance maximizing cell adhesion while preserving cerebral blood flow by monitoring cell engraftment in real time. MR imaging, with its exquisite spatial resolution, appears most suited for that purpose (1,14). MR imaging provides valuable information about the location of engraftment and migration and can potentially provide information about how well cells traffic to MR imaging-visible lesions. Furthermore, given the safety concerns that have been raised with this approach, additional monitoring techniques could be considered to measure changes in blood flow and tissue oxygenation, including laser Doppler (9), near-infrared spectroscopy (35), or MR imaging-based methods such as arterial spin labeling (36).

Acknowledgments: The authors thank Mary McAllister, MA, for editorial assistance and Mirosław Janowski, MD, PhD, for help with statistical analysis.

Disclosures of Potential Conflicts of Interest:

M.G. No potential conflicts of interest to disclose. **I.O.** No potential conflicts of interest to disclose. **J.W.** No potential conflicts of interest to disclose. **S.G.** No potential conflicts of interest to disclose. **H.K.** No potential conflicts of interest to disclose. **M.L.** Financial activities related to the present article: none to disclose. Financial activities not related to the present article: is a paid consultant for Geron; receives royalties from Lippincott; receives travel/accommodations/meeting expenses from Glaxo-Smith-Kline. Other relationships: none to disclose. **A.A.G.** No potential conflicts of interest to disclose. **A.B.** No potential conflicts of interest to disclose. **D.A.K.** Financial activities related to the present article: none to disclose. Financial activities not related to the present article: institution receives money for consultancy from Teva Pharmaceuticals and Nerveda; receives money for a patent (planned, pending or issued) from Nerveda; institution has stock/stock options in Biogen Idec; institution receives travel/accommodations/meeting expenses from Teva Neuroscience, Novartis, and Biogen. Other relationships: none to disclose. **A.L.** Financial activities related to the present article: none to disclose. Financial activities not related to the present article: re-

ceives royalties from Orion Genetics; has stock in Euveda Biosciences. Other relationships: none to disclose. **J.W.M.B.** Financial activities related to the present article: none to disclose. Financial activities not related to the present article: receives payment for lectures including service on speakers bureaus from various entities; receives royalties from Surgivision. Other relationships: none to disclose. **P.W.** No potential conflicts of interest to disclose.

References

- Berman SC, Galporthawela C, Gilad AA, Bulte JW, Walczak P. Long-term MR cell tracking of neural stem cells grafted in immunocompetent versus immunodeficient mice reveals distinct differences in contrast between live and dead cells. *Magn Reson Med* 2011;65(2):564–574.
- Sahni V, Kessler JA. Stem cell therapies for spinal cord injury. *Nat Rev Neurol* 2010;6(7):363–372.
- Winkler C, Kirik D, Björklund A. Cell transplantation in Parkinson's disease: how can we make it work? *Trends Neurosci* 2005;28(2):86–92.
- Janowski M, Walczak P, Date I. Intravenous route of cell delivery for treatment of neurological disorders: a meta-analysis of preclinical results. *Stem Cells Dev* 2010;19(1):5–16.
- Kraitchman DL, Tatsumi M, Gilson WD, et al. Dynamic imaging of allogeneic mesenchymal stem cells trafficking to myocardial infarction. *Circulation* 2005;112(10):1451–1461.
- Li L, Jiang Q, Ding G, et al. Effects of administration route on migration and distribution of neural progenitor cells transplanted into rats with focal cerebral ischemia: an MRI study. *J Cereb Blood Flow Metab* 2010;30(3):653–662.
- Shen LH, Li Y, Chen J, et al. Intracarotid transplantation of bone marrow stromal cells increases axon-myelin remodeling after stroke. *Neuroscience* 2006;137(2):393–399.
- Mahmood A, Lu D, Wang L, Li Y, Lu M, Chopp M. Treatment of traumatic brain injury in female rats with intravenous administration of bone marrow stromal cells. *Neurosurgery* 2001;49(5):1196–1203; discussion 1203–1204.
- Walczak P, Zhang J, Gilad AA, et al. Dual-modality monitoring of targeted intraarterial delivery of mesenchymal stem cells after transient ischemia. *Stroke* 2008;39(5):1569–1574.
- Pendharkar AV, Chua JY, Andres RH, et al. Biodistribution of neural stem cells after intravascular therapy for hypoxic-ischemia. *Stroke* 2010;41(9):2064–2070.
- Guzman R, De Los Angeles A, Cheshier S, et al. Intracarotid injection of fluorescence activated cell-sorted CD49d-positive neural stem cells improves targeted cell delivery and behavior after stroke in a mouse stroke model. *Stroke* 2008;39(4):1300–1306.
- Engelhardt B. Molecular mechanisms involved in T cell migration across the blood-brain barrier. *J Neural Transm* 2006;113(4):477–485.
- Yednock TA, Cannon C, Fritz LC, Sanchez-Madrid F, Steinman L, Karin N. Prevention of experimental autoimmune encephalomyelitis by antibodies against $\alpha 4 \beta 1$ integrin. *Nature* 1992;356(6364):63–66.
- Karussis D, Karageorgiou C, Vaknin-Dembinsky A, et al. Safety and immunological effects of mesenchymal stem cell transplantation in patients with multiple sclerosis and amyotrophic lateral sclerosis. *Arch Neurol* 2010;67(10):1187–1194.
- Barnett BP, Arepally A, Karmarkar PV, et al. Magnetic resonance-guided, real-time targeted delivery and imaging of magnetocapsules immunoprotecting pancreatic islet cells. *Nat Med* 2007;13(8):986–991.
- Karmarkar PV, Kraitchman DL, Izbudak I, et al. MR-trackable intramyocardial injection catheter. *Magn Reson Med* 2004;51(6):1163–1172.
- Rey S, Lee K, Wang CJ, et al. Synergistic effect of HIF-1 α gene therapy and HIF-1-activated bone marrow-derived angiogenic cells in a mouse model of limb ischemia. *Proc Natl Acad Sci U S A* 2009;106(48):20399–20404.
- Walczak P, All AH, Rumpal N, et al. Human glial-restricted progenitors survive, proliferate, and preserve electrophysiological function in rats with focal inflammatory spinal cord demyelination. *Glia* 2011;59(3):499–510.
- Correia AS, Anisimov SV, Li JY, Brundin P. Stem cell-based therapy for Parkinson's disease. *Ann Med* 2005;37(7):487–498.
- Capetian P, Knoth R, Maciaczyk J, et al. Histological findings on fetal striatal grafts in a Huntington's disease patient early after transplantation. *Neuroscience* 2009;160(3):661–675.
- Mazzini L, Mareschi K, Ferrero I, et al. Autologous mesenchymal stem cells: clinical applications in amyotrophic lateral sclerosis. *Neurol Res* 2006;28(5):523–526.
- Kelly S, Bliss TM, Shah AK, et al. Transplanted human fetal neural stem cells survive, migrate, and differentiate in ischemic rat cerebral cortex. *Proc Natl Acad Sci U S A* 2004;101(32):11839–11844.
- Calabrese M, Battaglini M, Giorgio A, et al. Imaging distribution and frequency of cortical lesions in patients with multiple

- sclerosis. *Neurology* 2010;75(14):1234-1240.
24. Boncoraglio GB, Bersano A, Candelise L, Reynolds BA, Parati EA. Stem cell transplantation for ischemic stroke. *Cochrane Database Syst Rev* 2010 (9):CD007231.
 25. Li Y, Chen J, Chen XG, et al. Human marrow stromal cell therapy for stroke in rat: neurotrophins and functional recovery. *Neurology* 2002;59(4):514-523.
 26. Fischer UM, Harting MT, Jimenez F, et al. Pulmonary passage is a major obstacle for intravenous stem cell delivery: the pulmonary first-pass effect. *Stem Cells Dev* 2009;18(5):683-692.
 27. Semon JA, Nagy LH, Llamas CB, Tucker HA, Lee RH, Prockop DJ. Integrin expression and integrin-mediated adhesion in vitro of human multipotent stromal cells (MSCs) to endothelial cells from various blood vessels. *Cell Tissue Res* 2010;341(1):147-158.
 28. Prowse AB, Chong F, Gray PP, Munro TP. Stem cell integrins: implications for ex-vivo culture and cellular therapies. *Stem Cell Res (Amst)* 2011;6(1):1-12.
 29. Subileau EA, Rezaie P, Davies HA, et al. Expression of chemokines and their receptors by human brain endothelium: implications for multiple sclerosis. *J Neuropathol Exp Neurol* 2009;68(3):227-240.
 30. Blann A, Kumar P, Krupinski J, McCollum C, Beevers DG, Lip GYH. Soluble intercellular adhesion molecule-1, E-selectin, vascular cell adhesion molecule-1 and von Willebrand factor in stroke. *Blood Coagul Fibrinolysis* 1999;10(5):277-284.
 31. Ceradini DJ, Kulkarni AR, Callaghan MJ, et al. Progenitor cell trafficking is regulated by hypoxic gradients through HIF-1 induction of SDF-1. *Nat Med* 2004;10(8):858-864.
 32. Janowski M. Functional diversity of SDF-1 splicing variants. *Cell Adhes Migr* 2009;3(3):243-249.
 33. Belmadani A, Tran PB, Ren D, Miller RJ. Chemokines regulate the migration of neural progenitors to sites of neuroinflammation. *J Neurosci* 2006;26(12):3182-3191.
 34. Chua JY, Guzman R. Intraarterial neural stem cell delivery does not result in reduction of CBF and micro strokes. *Stroke* 2010;41(4):E354.
 35. McCormick PW, Stewart M, Goetting MG, Balakrishnan G. Regional cerebrovascular oxygen saturation measured by optical spectroscopy in humans. *Stroke* 1991;22(5):596-602.
 36. Lu H, Donahue MJ, van Zijl PC. Detrimental effects of BOLD signal in arterial spin labeling fMRI at high field strength. *Magn Reson Med* 2006;56(3):546-552.